

Probing Exotic Scalar Fields by Utilizing the GPS System

Yu Li¹

Instructor: Niayesh Afshordi², Conner Dailey²

¹Faculty of Mathematics, University of Waterloo

²University of Waterloo & Perimeter Institute for Theoretical Physics

Canadian Astroparticle Summer Student Talk Competition, Aug 2022

Table of Contents

- 1 Motivation
- 2 Working Principle
- 3 Results so far
- 4 More things to work on
- 5 References

Table of Contents

- 1 Motivation
- 2 Working Principle
- 3 Results so far
- 4 More things to work on
- 5 References

- Some beyond-standard-model theories, such as the Axi-Higgs model[4], suggest the existence of **exotic low-mass scalar fields** that couple to matter.

- Some beyond-standard-model theories, such as the Axi-Higgs model[4], suggest the existence of **exotic low-mass scalar fields** that couple to matter.
- During high-energy astrophysical events such as the binary neutron star (BNS) mergers, these scalar fields may be emitted as radiation.

- Some beyond-standard-model theories, such as the Axi-Higgs model[4], suggest the existence of **exotic low-mass scalar fields** that couple to matter.
- During high-energy astrophysical events such as the binary neutron star (BNS) mergers, these scalar fields may be emitted as radiation.
- Our goal is to utilize the GPS system to detect such scalar radiations.

Table of Contents

- 1 Motivation
- 2 Working Principle**
- 3 Results so far
- 4 More things to work on
- 5 References

Working Principle

- GPS satellites have atomic clocks onboard to correct for relativistic effects.

Working Principle

- GPS satellites have atomic clocks onboard to correct for relativistic effects.
- Therefore, the GPS constellation forms an array of quantum sensors around the globe.

Working Principle

- The exotic scalar fields can effectively generate signals in quantum sensors via "portals" between the exotic fields and standard model particles and fields[1].

Working Principle

- The exotic scalar fields can effectively generate signals in quantum sensors via "portals" between the exotic fields and standard model particles and fields[1].
- Portals are a phenomenological gauge-invariant collection of standard model operators coupled with operators from the scalar sector[1].

Linear Interaction Lagrangian of an Atomic Clock

$$\mathcal{L}_{\text{clk}}^{(1)} = \sqrt{4\pi}/E_{\text{pl}}(-d_{m_e}m_e c^2 \bar{\psi}_e \psi_e + d_e F_{\mu\nu}^2/4)\phi$$

Quadratic Interaction Lagrangian of an Atomic Clock

$$\mathcal{L}_{\text{clk}}^{(2)} = (-m_e c^2 \bar{\psi}_e \psi_e / \Lambda_{m_e}^2 + F_{\mu\nu}^2 / (4\Lambda_\alpha^2))\phi^2$$

Here, ϕ is the scalar field, ψ_e is the electron bi-spinor, $F_{\mu\nu}$ is the Faraday tensor, E_{pl} is the Plank energy, and d_e , d_{m_e} , Λ_{m_e} , Λ_α are coupling constants.

Working Principle

- The interaction between ϕ and the atomic clocks effectively alter fundamental constants, such as the electron mass m_e and the fine-structure constants α [2], thus imprinting measurable signals in atomic clocks.

Working Principle

- The interaction between ϕ and the atomic clocks effectively alter fundamental constants, such as the electron mass m_e and the fine-structure constants α [2], thus imprinting measurable signals in atomic clocks.
- In the sensitivity analysis section of our previous paper[1], we have shown that the current generation of atomic clocks is sensitive to the quadratic portal $\mathcal{L}_{\text{clk}}^{(2)}$.

Working Principle

- The interaction between ϕ and the atomic clocks effectively alter fundamental constants, such as the electron mass m_e and the fine-structure constants α [2], thus imprinting measurable signals in atomic clocks.
- In the sensitivity analysis section of our previous paper[1], we have shown that the current generation of atomic clocks is sensitive to the quadratic portal $\mathcal{L}_{\text{clk}}^{(2)}$.
- In practice, we can see the signal via accessing the satellite clock data.

Working Principle

- The interaction between ϕ and the atomic clocks effectively alter fundamental constants, such as the electron mass m_e and the fine-structure constants α [2], thus imprinting measurable signals in atomic clocks.
- In the sensitivity analysis section of our previous paper[1], we have shown that the current generation of atomic clocks is sensitive to the quadratic portal $\mathcal{L}_{\text{clk}}^{(2)}$.
- In practice, we can see the signal via accessing the satellite clock data.
- The satellite data is in the form {Epoch time (J2000 seconds), 0 for some reason, clock data in (meters), formal error in (meters), SVN name}.

Working Principle

- The interaction between ϕ and the atomic clocks effectively alter fundamental constants, such as the electron mass m_e and the fine-structure constants α [2], thus imprinting measurable signals in atomic clocks.
- In the sensitivity analysis section of our previous paper[1], we have shown that the current generation of atomic clocks is sensitive to the quadratic portal $\mathcal{L}_{\text{clk}}^{(2)}$.
- In practice, we can see the signal via accessing the satellite clock data.
- The satellite data is in the form {Epoch time (J2000 seconds), 0 for some reason, clock data in (meters), formal error in (meters), SVN name}.
- By differencing the clock data, we will get the perturbations on the clocks. If there is an extra perturbation in addition to the background noise, it can possibly be the signal we are looking for.

Note:

The sampling rate of the publicly-accessible satellite data is too low for our purpose. Our group has a connection with the NASA JPL team. With their permission, we are able to use the high-sampling-rate satellite data.

Working Principle

This detection method has a few advantages:

- The facility it utilizes already exists, meaning that there is no need to build expensive new apparatus.

Working Principle

This detection method has a few advantages:

- The facility it utilizes already exists, meaning that there is no need to build expensive new apparatus.
- Our previous calculations[1] show that other forms of signal, such as the gravitational wave signal, are shielded from the atomic clocks on the GPS, thanks to their low sampling rates.

Working Principle

This detection method has a few advantages:

- The facility it utilizes already exists, meaning that there is no need to build expensive new apparatus.
- Our previous calculations[1] show that other forms of signal, such as the gravitational wave signal, are shielded from the atomic clocks on the GPS, thanks to their low sampling rates.
- About 20 years' worth of GPS data is available in the database, so we can trace back in time to search for low-mass scalar field bursts, by correlating to LIGO data or short gamma-ray bursts.

Working Principle

This detection method has a few advantages:

- The facility it utilizes already exists, meaning that there is no need to build expensive new apparatus.
- Our previous calculations[1] show that other forms of signal, such as the gravitational wave signal, are shielded from the atomic clocks on the GPS, thanks to their low sampling rates.
- About 20 years' worth of GPS data is available in the database, so we can trace back in time to search for low-mass scalar field bursts, by correlating to LIGO data or short gamma-ray bursts.
- If no scalar signal is detected, certain theoretical constraints then need to be applied to those beyond-standard-model theories.

Table of Contents

- 1 Motivation
- 2 Working Principle
- 3 Results so far**
- 4 More things to work on
- 5 References

Results so far

In the previous paper[1], we considered a monochromatic Gaussian wave packet of the scalar signal. That signal would look like a straight line with negative slope in the time-frequency space:

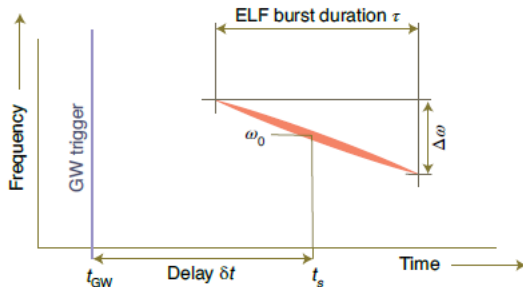


Figure: Dailey, C., et al. (2020). Time–frequency decomposition for power spectrum of a scalar field signal at a sensor. *Nature Astronomy*.

Results so far

- However, in an actual BNS event, the signal is not monochromatic, Instead, the emission waveform should be closely related to the inspiral frequencies of the merging bodies. Then, it would be modified by propagation effects.

Results so far

- However, in an actual BNS event, the signal is not monochromatic, Instead, the emission waveform should be closely related to the inspiral frequencies of the merging bodies. Then, it would be modified by propagation effects.
- By considering the quadrupole radiations[3], we derived the following expression for the waveform:

Waveform derived from inspiral frequencies

$$\phi(t, r) = \int \frac{A}{f^{7/6}} e^{\Psi} df$$

where the phase Ψ is given by:

$$\Psi(f, t, r) = ir \left(\sqrt{\left(\frac{2\pi f}{c}\right)^2 - \left(\frac{mc}{\hbar}\right)^2} - \frac{2\pi f}{c} \right) - 2i\pi ft + \frac{3i}{128} \left(\frac{\pi MGf}{c^3}\right)^{-5/3}$$

Results so far

Here, A is a constant amplitude with appropriate dimensions that depends on the strength of the coupling, m is the mass of the scalar field, M is the chirp mass of the merging event, r is the distance to the event, and t is the time since the gravitational wave trigger.

Results so far

By using saddle points approximations to estimate the waveform, we expect this signal would look like the following curve in time-frequency space (time is measured since the gravitational wave trigger):

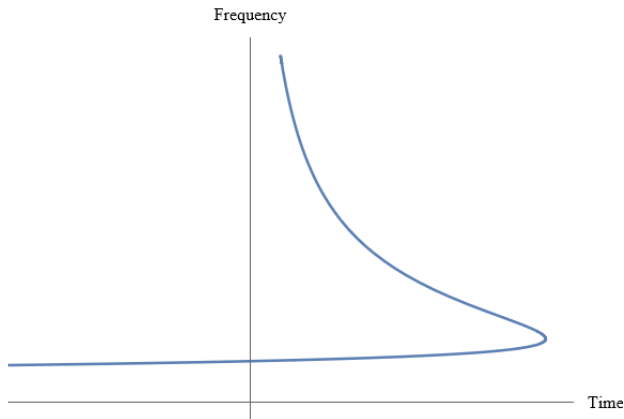


Figure: The qualitative shape of a typical waveform.

- Note that since the satellite clocks have a fixed sampling rate (1 Hz), in the spectrogram of an actual signal, we may not be able to see the whole curve in the last figure. Only part of the curve that fits in the sampling window can appear in the spectrogram. We will most likely see the lower (flat) part of the curve.

- Note that since the satellite clocks have a fixed sampling rate (1 Hz), in the spectrogram of an actual signal, we may not be able to see the whole curve in the last figure. Only part of the curve that fits in the sampling window can appear in the spectrogram. We will most likely see the lower (flat) part of the curve.
- Different frequency components are emitted at different stages of the inspiral. Also, since the scalar field is not mass-less, different frequency components travel at different speeds. The peak in the last figure (mostly delayed component) is a result of the balance of these two effects.

The following log-log animated plots show how the waveform in time-frequency space changes with respect to the mass of the scalar field and the distance of the event:

- mass: https://drive.google.com/file/d/1KypHeCmHApJJ3Ab9v7vgGwlInnHMg_fFD/view?usp=sharing

The following log-log animated plots show how the waveform in time-frequency space changes with respect to the mass of the scalar field and the distance of the event:

- mass: https://drive.google.com/file/d/1KypHeCmHApJJ3Ab9v7vgGwlnnHMg_fFD/view?usp=sharing
- distance: <https://drive.google.com/file/d/1qCI-a17gbZfYU8-aMSR3P0ymNgmnVXGG/view?usp=sharing>

Results so far

- Using the above waveform, we can calculate the spectral density of the scalar signal.

Results so far

- Using the above waveform, we can calculate the spectral density of the scalar signal.
- If the observation interval is infinite, the scalar density is simply the norm square of the Fourier amplitude: $|A/f^{7/6}|^2 = A^2/f^{7/3}$.

Results so far

- Using the above waveform, we can calculate the spectral density of the scalar signal.
- If the observation interval is infinite, the scalar density is simply the norm square of the Fourier amplitude: $|A/f^{7/6}|^2 = A^2/f^{7/3}$.
- However, in a realistic situation, the observation interval is some finite time T . In such a case, we must do a "partial Fourier transform" (here we use angular frequency $\omega = 2\pi f$ as a variable):

$$P_s(\omega) = |\psi'(\omega)|^2$$

where

$$\psi'(\omega) = \int_{-T/2}^{T/2} e^{i\omega t} \phi(t, r) dt$$

Results so far

Using the expression for ϕ , the above equation simplifies to:

Spectral density of the waveform

$$P_s(\omega) = |\psi'(\omega)|^2$$

where

$$\psi'(\omega) = \int \frac{A}{\omega'^{7/6}} \exp\left(\frac{3i}{128} \left(\frac{MG\omega'}{2c^3}\right)^{-5/3} + ir \left(\sqrt{\left(\frac{\omega'}{c}\right)^2 - \left(\frac{mc}{\hbar}\right)^2} - \frac{\omega'}{c}\right)\right) T \operatorname{sinc}\left(\frac{1}{2} T(\omega - \omega')\right) d\omega'$$

Results so far

Using saddle point approximations, we plot the spectral density of the signal for $T = 30000000\text{s}$ (we used $A = 1$ for the plot):

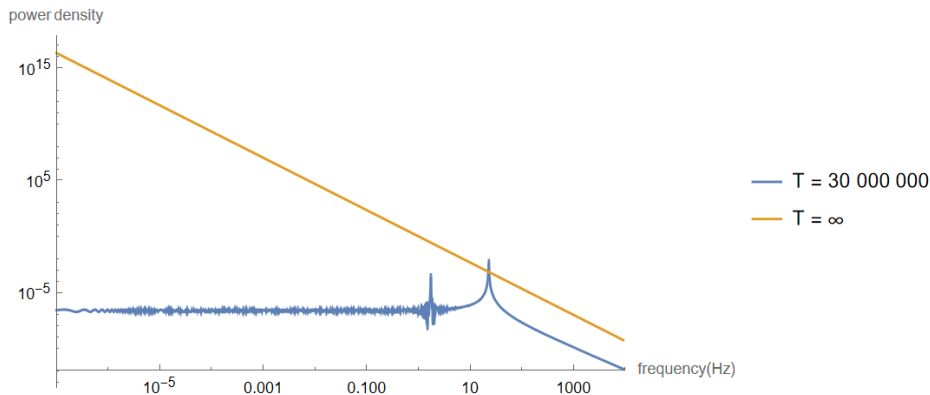


Figure: The spectral density of a signal when $T = 30000000\text{s}$.

Results so far

- In this plot we have used the parameters $r = 2.234 \times 10^{24} \text{m}$, $M = 1.99 \times 10^{30} \text{kg}$, $m = 9.78 \times 10^{-56} \text{kg}$, which are typical for a BNS event and the scalar field we are considering.

Results so far

- In this plot we have used the parameters $r = 2.234 \times 10^{24} \text{m}$, $M = 1.99 \times 10^{30} \text{kg}$, $m = 9.78 \times 10^{-56} \text{kg}$, which are typical for a BNS event and the scalar field we are considering.
- It can be seen that the power density for $T = 300000000 \text{s}$ is less than that of $T = \infty$ for most frequencies, which is reasonable, since the more time you observe, the more power you will receive.

Results so far

- In this plot we have used the parameters $r = 2.234 \times 10^{24} \text{m}$, $M = 1.99 \times 10^{30} \text{kg}$, $m = 9.78 \times 10^{-56} \text{kg}$, which are typical for a BNS event and the scalar field we are considering.
- It can be seen that the power density for $T = 30000000 \text{s}$ is less than that of $T = \infty$ for most frequencies, which is reasonable, since the more time you observe, the more power you will receive.
- Under certain circumstances ($m = 0$), it can be shown that the peaks (which are the saddle points of the wave phase) are closely related to the average value of the inspiral frequency of a BNS event $\Omega(t) = \left(\frac{5}{256} \frac{1}{t_c - t} \right)^{3/8} \left(\frac{MG}{c^3} \right)^{-5/8} [3]$. In a more general case, an analytic expression cannot be derived. But we still conjecture that the peaks are related to the average of the inspiral frequency. This is reasonable since from the expression of $\Omega(t)$, we see that $\Omega(t)$ is around its average value most of the time during the observation period (and suddenly blows up). Hence, you will receive the most power around that frequency.

Results so far

The next part is the background noise analysis from satellite data.

- As we have mentioned, we can get the pre-event perturbations on the atomic clocks from differencing the pre-event clock data. Note that the clock data is in meters (so we need to divide by c to get the usual clock data in seconds).

Results so far

The next part is the background noise analysis from satellite data.

- As we have mentioned, we can get the pre-event perturbations on the atomic clocks from differencing the pre-event clock data. Note that the clock data is in meters (so we need to divide by c to get the usual clock data in seconds).
- Then, using Discrete Fourier Transform, we can evaluate the spectral density of the background noise. Here is a plot of it (we use angular frequency ω as a variable):

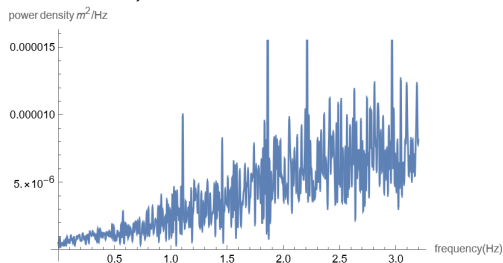


Figure: The spectral density of the back ground noise.

- We have selected the data from the satellite GPS71 to produce this plot. According to satellite experts, the data from this particular satellite is in general more reliable.

- We have selected the data from the satellite GPS71 to produce this plot. According to satellite experts, the data from this particular satellite is in general more reliable.
- We only plot the spectral density for angular frequency ω between 0 and 3.2Hz. This is because the sampling rate of the satellite is 1Hz, so any spectral gram produced from the satellite data can only show frequencies f between 0 and 0.5Hz (the Nyquist frequency), hence $\omega = 2\pi f$ should be between 0 and π .

Table of Contents

- 1 Motivation
- 2 Working Principle
- 3 Results so far
- 4 More things to work on**
- 5 References

More things to work on

- A more delicate examination on the production mechanism (i.e. theoretical models such as the Axi-Higgs model) need to be done in order to determine the relation between the coupling strength and the wave amplitude A . We need to use A to normalize the waveform in order to determine the signal-to-noise ratio as a function of frequency. This will tell us how strong the coupling needs to be in order to let the signal be visible, and which part of the signal is visible on the detector.





More things to work on

- A more delicate examination on the production mechanism (i.e. theoretical models such as the Axi-Higgs model) need to be done in order to determine the relation between the coupling strength and the wave amplitude A . We need to use A to normalize the waveform in order to determine the signal-to-noise ratio as a function of frequency. This will tell us how strong the coupling needs to be in order to let the signal be visible, and which part of the signal is visible on the detector.
- We have only considered quadrupole radiations so far. We will use the same methodology to examine dipole radiations. It is most likely that the power of the denominator in the waveform need to be changed for dipole radiations.

- Another interesting question is how well the timing information from the GPS network can be used to localize the event in the sky. The scalar field we are considering travels so fast that the time it takes to travel through the entire GPS constellation is slightly less than the sampling interval of the clocks. However, so inference may still be done to estimate the direction of the event (we are still working on this to see if this is possible).

Table of Contents

- 1 Motivation
- 2 Working Principle
- 3 Results so far
- 4 More things to work on
- 5 References**

-  Conner Dailey, C. B., et al. (2020). Quantum sensor networks as exotic field telescopes for multi-messenger astronomy. *Nature Astronomy*.
-  Derevianko, A. Pospelov, M. (2014). Hunting for topological dark matter with atomic clocks. *Nature Physics* 10, 933.
-  Isoyama, S., Sturani, R., Nakano, H. (2021). Post-Newtonian templates for gravitational waves from compact binary inspirals. *Handbook of Gravitational Wave Astronomy*.
-  Leo WH Fung, L. L.-C.-H., et al. (2021). Axi-Higgs Cosmology. arXiv:2102.11257